



## Review article

## Protonic ceramic electrochemical cells: Opportunities and challenges for ammonia synthesis

Qinyi Hu<sup>a,b</sup>, Chuan Tian<sup>c</sup>, Di Bao<sup>a</sup>, Haixia Zhong<sup>a,b,\*</sup>, Xinbo Zhang<sup>a,b,\*</sup><sup>a</sup> State Key Laboratory of Rare Earth Resource Utilization, Changchun Institute of Applied Chemistry, Chinese Academy of Sciences, Changchun 130022, China<sup>b</sup> School of Applied Chemistry and Engineering, University of Science and Technology of China, Hefei 230026, China<sup>c</sup> Jilin Normal University, Key Laboratory of Preparation and Applications of Environmentally Friendly Materials, Ministry of Education, Changchun, Jilin 130103, China

## ARTICLE INFO

## Keywords:

Protonic ceramic electrochemical cells  
Ammonia synthesis  
Perovskite oxides

## ABSTRACT

Electrochemical ammonia synthesis is being widely investigated to couple with renewable electricity for future sustainable ammonia production. Protonic ceramic electrochemical cells (PCECs) possess superior energy transfer efficiency and remarkable flexibility to produce high-demand chemicals such as H<sub>2</sub>, CH<sub>4</sub>, and NH<sub>3</sub> from readily available feedstocks (e.g., H<sub>2</sub>O, CO<sub>2</sub>, N<sub>2</sub>). Despite recent advances that have been established, the research for the high-efficiency PCECs for practical ammonia synthesis continues. In this review, we summarized the recent progress of PCECs for ammonia synthesis. First, we briefly introduce the basic mechanisms and protocols of the ammonia synthesis. Then, we systemically introduce the cell configurations, representative electrolytes and electrodes of PCECs for the ammonia synthesis. We highlight the strategies to tune the ion/electron mobility and the catalytic performance, which are related to the defect structures and redox properties of the electrolyte/electrode, and the opportunities for next-generation ammonia synthesis. Finally, perspectives on ammonia synthesis in PCECs are proposed concerning the current challenges.

## 1. Introduction

Ammonia plays an important role in agriculture and the chemical industry with an annual production of around 170 million tonnes around the world. Additionally, ammonia is also a potential carbon-free energy carrier due to its high energy density (4 kWh kg<sup>-1</sup>) and easy liquefaction (10 atm at ambient temperature) for storage and transportation [1–3]. Nowadays, ammonia is mainly produced from nitrogen and hydrogen through the traditional Haber-Bosch process (over 96%) using the magnetite-based fused iron catalyst (Fe<sub>3</sub>O<sub>4</sub>/Fe<sub>1-x</sub>O + Al<sub>2</sub>O<sub>3</sub> + K<sub>2</sub>O + CaO + ...) with enormous energy consumption (1–2% of the energy output of the whole world) and over 1% of global carbon emissions [4,5]. For enhancing the nitrogen conversion efficiency, harsh reaction conditions of particularly high pressure (10–30 Mpa) are needed, imposing high requirements for reactors. The ambient pressure electrochemical nitrogen reduction reaction (eNRR) to ammonia, driven by renewable electricity, has been extensively researched as a potential sustainable ammonia production technique [6,7].

Protonic ceramic electrochemical cells (PCECs) have been proven to be a promising technology for value-added chemical synthesis. The high energy utilization efficiency is presented by PCECs owing to the

favorable thermodynamic and kinetics at intermediate temperatures (400–650 °C) [8], which can be also flexibly integrated with other distributed renewable energy systems (Fig. 1). For instance, PCECs have made significant progress in the direct conversion of water to hydrogen and ethane to ethylene [9–14]. Recently, numerous efforts have focused on the development of PCECs for advancing environmentally friendly ammonia synthesis processes. However, due to the inert feature of nitrogen (N≡N: 941 kJ mol<sup>-1</sup>) and the fast side reactions, the current ammonia efficiency including selectivity and yield rate, is far behind the requirement of the practical application [7].

Despite offering the opportunity for efficient ammonia synthesis, PCECs are still at a nascent stage and progress slowly, wherein high catalytic activity electrodes and high proton/oxygen ion conducting ceramic electrolytes are essential components. Moreover, understanding ascertaining the rate-determining step (RDS) and the genuine eNRR active sites for the multitude of potential reaction pathways is ongoing for performance improvement as well. Nevertheless, it is a long-standing goal to develop robust PCECs for realizing efficient and stable ammonia synthesis on a wider scale. In this review, advances of PCECs for the ammonia synthesis are summarized at the key material and cell level. First, the main difficulties, mechanisms and protocols of electrochemical ammonia synthesis are briefly introduced. Then,

\* Corresponding author at: State Key Laboratory of Rare Earth Resource Utilization, Changchun Institute of Applied Chemistry, Chinese Academy of Sciences, Changchun 130022, China

E-mail addresses: [hxzhong@ciac.ac.cn](mailto:hxzhong@ciac.ac.cn) (H. Zhong), [xbzhang@ciac.ac.cn](mailto:xbzhang@ciac.ac.cn) (X. Zhang).

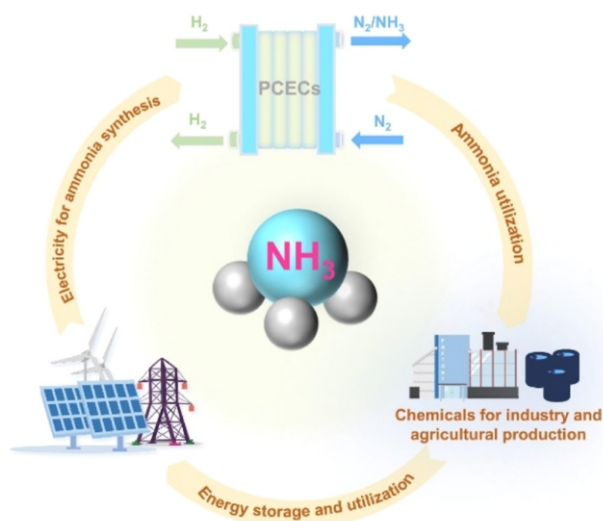


Fig. 1. Schematic illustration of the ammonia synthesis process by PCECs.

typical electrodes and electrolytes of PCECs are systemically discussed. Therefore, effective strategies for material design and property modification as well as an insightful understanding of the reaction mechanism are emphasized. Finally, perspectives on ammonia synthesis in PCECs are proposed with respect to the current challenges. This review aims to provide a guide for the further development of PCECs in ammonia synthesis technology.

## 2. Protocols for electrochemical ammonia synthesis

### 2.1. Reaction mechanism

In general, the nitrogen reduction process consists of three main parts (Fig. 2a): i) adsorption of nitrogen molecules on the catalyst surfaces; ii) activation of absorbed nitrogen molecules and the subsequent hydrogenation and electron transfer process on the catalytic surface; iii) desorption of ammonia molecules or by-products ( $N_2H_2$ ,  $N_2H_4$ ) from the catalyst surfaces. Here, the transport of protons and electrons through the bulk electrolyte is not considered for the above NRR process. Over the past few decades, several NRR pathways have been proposed in heterogeneous catalytic systems, such as the dissociative mechanism, associative mechanism, and Mars-van Krevelen mechanism [6] (Fig. 2b). Despite with the catalyst, electrochemical reaction processes are also related to the applied conditions because of the complex electron transfer steps and numerous possible reaction intermediates. For example, Jun and Back found that various limiting potentials ( $U_L$ ,  $U_L = -\Delta G_{max}/e$ ) correspond to different reaction pathways on the Ru catalyst [15]. When  $U_L$  was between  $-0.71$  V and  $-0.68$  V, the associative mechanism was dominant (Fig. 2c), while the dissociation of  $*NNH_2$ ,  $*NHNH_2$ ,  $*NH_2NH_2$  was thermodynamically feasible under the potentials of  $< -0.71$  V.

#### 2.1.1. Dissociative mechanism

Nitrogen molecules are first absorbed on the catalyst surface and broken up into two isolated nitrogen atoms. The nitrogen atoms are then converted into ammonia molecules via a stepwise hydrogenation process and ammonia detachment from the catalyst surface. Due to the high energy barrier to overcoming the sluggish dissociation of the triple bond, the nitrogen dissociation on the surface is the RDS and is normally found in high-temperature catalytic systems. For instance, the traditional Haber-Bosch process is a typical example, exhibiting a higher rate constant than that for the associative process at industry operating conditions [16].

#### 2.1.2. Associative mechanism

The associative mechanism was proposed on the transition metal surfaces by Nørskov and coworkers [17]. Different from the dissociative pathway, the triple bond of nitrogen is sequentially ruptured with the additive reaction of hydrogen atoms. The cleavage of nitrogen molecules is accompanied by the production of the first ammonia molecule in the associative pathway, which is mainly observed in the electrochemical process at low temperatures. This mechanism can be further divided into alternating and distal pathways according to the following different hydrogenation sequences. The alternating pathway involves the sequential addition of hydrogen atoms by each of two nitrogen atoms until the first ammonia molecule is released. In terms of the distal pathway, hydrogen atoms initially combine with the nitrogen atom situated the farthest from the catalyst surface to form the first ammonia molecule. Thereafter the nitrogen atom adsorbed on the catalyst surface continues to be hydrogenated. Thus, promoting the activation of nitrogen molecules and modulating the interaction of the intermediates on the catalytic surface would be effective for the rapid nitrogen reduction reaction to ammonia.

#### 2.1.3. Mars-van Krevelen mechanism

Similar to the lattice oxygen mechanism (LOM) in the oxygen evolution reaction, lattice nitrogen atoms can also participate in NRR as the active sites which is referred to as the Mars-van Krevelen mechanism (MvK)[18]. This exchange behavior of lattice N and environment nitrogen is confirmed by nitrogen isotopic exchange experiments [19]. As present in Fig. 2d, two general nitrogen-filling pathways have been proposed. The first is a so-called dissociative mechanism (left figure) in which an N vacancy is filled with a nitrogen molecule to form a lattice N atom and a neighboring surface N atom. When the filling of the N vacancies is an endothermic step, the N atoms are replenished by the alternative pathway (right figure). In this way, the N vacancies are filled with nitrogen as dimers rather than individual sites [20,21]. Thus, this nitrogen vacancy-involved NRR process can bypass the linear scaling of different adsorbents, which is favorable for accelerating NRR kinetics. However, vacancy-filling with environment nitrogen is difficult and will result in structural instability.

### 2.2. Ammonia detection methods

Currently, the achieved rate of ammonia synthesis is relatively low ( $<10^{-7}$  mol  $s^{-1}$   $cm^{-2}$ ) due to the slow NRR kinetics. To eliminate false positive results from the potentially contaminated nitride and to ensure the reliability of the results, rigorous experimental protocols are essentially executed. Chorkendorff and coworkers proposed a rigorous procedure to quantify the true ammonia synthesis rate of catalysts [22]. For the whole experimental process, several details need to be particularly considered. First, the feed nitrogen for ammonia synthesis should be pretreated to completely remove nitrogen-containing impurities (e.g., NO,  $NO_2$ ,  $N_2O$  and extraneous  $NH_3$ ).  $NH_3$  and  $NO_2$  in the feed gas can be removed by passing through dilute  $H_2SO_4$  as they are soluble in water. And the residual NO of the feed gas after the above process can be reduced to  $N_2$  on the Cu-based catalysts (Cu-SSZ-13, Cu-SAPO-34, etc.) at 300 °C. Next, the catalysts themselves may be contaminated with foreign nitrides. To eliminate the interference of nitrogen compounds, it is necessary to perform the well-designed blank experiments at the operating potential under the Ar atmosphere and without the applied voltage under the  $N_2$  atmosphere, respectively. The ammonia detected should be an order of magnitude lower than under the  $N_2$  atmosphere with voltage applied. Typically,  $^{15}N$  isotope-labeled experiments are applied to check whether the ammonia is synthesized from  $N_2$  rather than other nitrides.  $^{15}NH_3$  and  $^{14}NH_3$  can be clearly and conveniently distinguished by the nuclear magnetic resonance (NMR) spectroscopy because the  $^{15}NH_3$  couples with an  $H^+$  to form  $^{15}NH_4^+$ , which shows a doublet peak with a spacing of 73 Hz, while the  $^{14}NH_4^+$  shows a triplet peak with a spacing of 52 Hz.

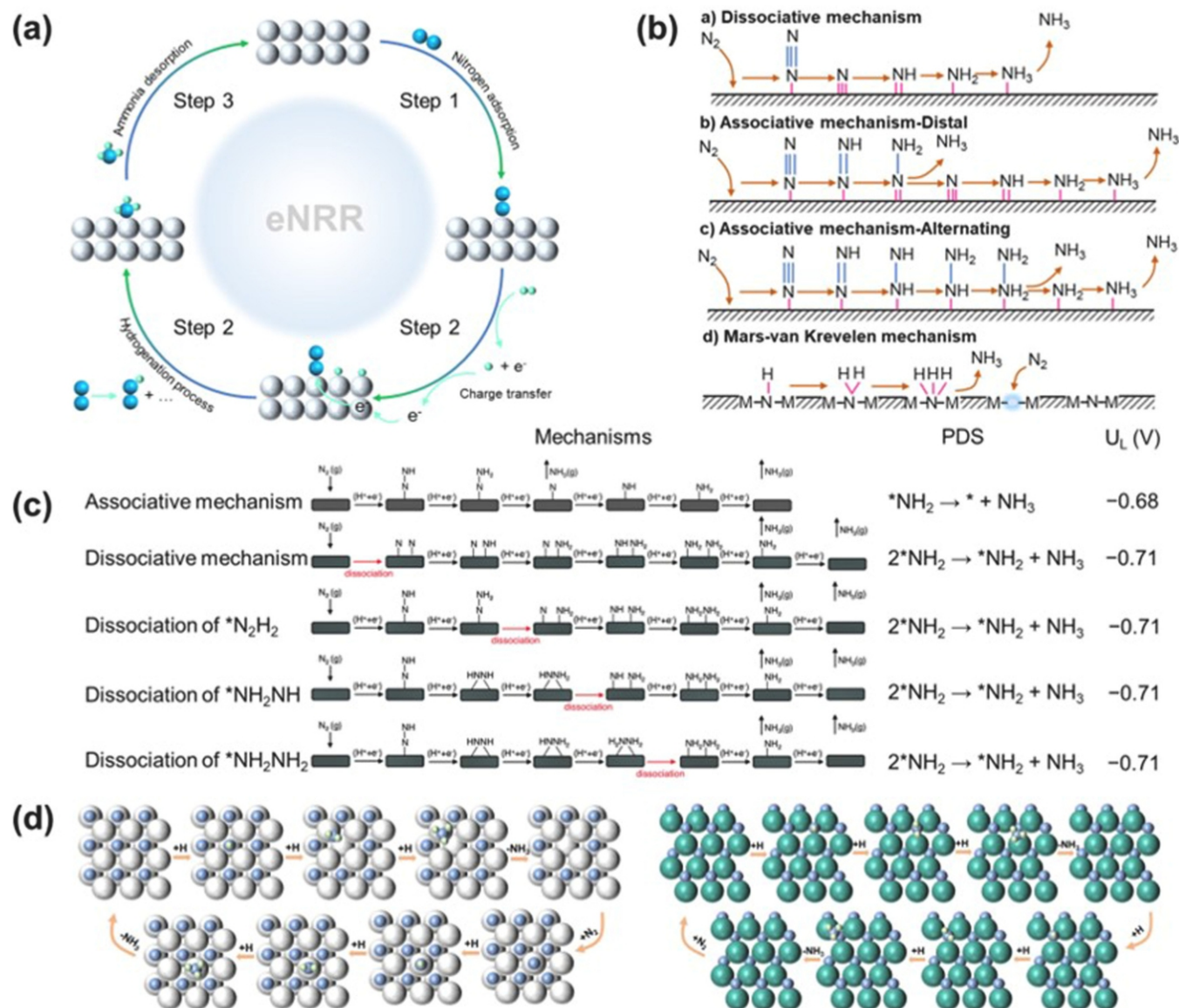


**Fig. 2.** (a) Reaction process of nitrogen reduction to ammonia. (b) Schematics of typical NRR mechanisms. (c) Reaction mechanisms and PDS on Ru with different  $U_L$ . (d) Nitrogen molecules replenishment pathways of Mars-van Krevelen mechanism.

(c) Reproduced with permission from ref. [15]. Copyright 2016, Royal Society of Chemistry. (d) Reproduced with permission from ref. [20]. Copyright 2016, Royal Society of Chemistry.

In order to accurately detect the ammonia content, various detection methods have been developed, such as spectrophotometry, ion chromatography, ion-selective electrodes, etc [23]. The indophenol blue method is mainly used for ammonia detection because of its convenience, accuracy, and wide detection range. Ammonia reacts with phenol and hypochlorite under alkaline conditions to form blue-colored indophenol which can be quantitatively detected by Ultraviolet and Visible Spectroscopy (UV-vis) at wavelengths between 630 nm and 650 nm. Sodium nitroprusside is added as a catalyst to facilitate the reaction and intensify the blue color. Citrate or ethylenediaminetetraacetic acid (EDTA) is also needed to be added as a buffer to stabilize the pH and as a complexing agent to prevent the precipitation of hydroxides and shield the influence of potential metal ions. However, the highly volatile and toxic ortho-chlorophenol is also produced during the whole reaction steps. Recently, the modified salicylate method is gradually becoming the main method for ammonia detection. In this reaction, the blue-green colored 5-aminosalicylate is formed by the reaction of salicylate, ammonia and hypochlorite under alkaline conditions [24].

### 2.3. Reaction enhancement principles

Stable triple bonds and non-polar molecular properties lead to nitrogen activation extremely difficult. The complex reaction intermediates and electron transfer steps result in a low faradaic efficiency (FE) of ammonia synthesis. Hence, the rational catalyst design is necessary to enhance the nitrogen activation and selective reduction process.

Over the past few decades, intense efforts have gone into finding suitable descriptors to guide the catalyst design. In 1920, Paul Sabatier qualitatively proposed the Sabatier principle, which stated that the ideal catalyst should have a moderate adsorption capacity for reactants. When the adsorption between catalysts and reactants is too strong, the reactants will be densely adsorbed on the surface of catalysts, resulting in the deactivation of the active sites [25]. On the other hand, it is difficult to capture enough reactant to drive the subsequent reaction if the adsorption is too weak. In 1969, Balandin proposed the volcano curves based on the Sabatier principle and attempted to quantify the adsorption capacity of reactants on catalysts. The volcano curves

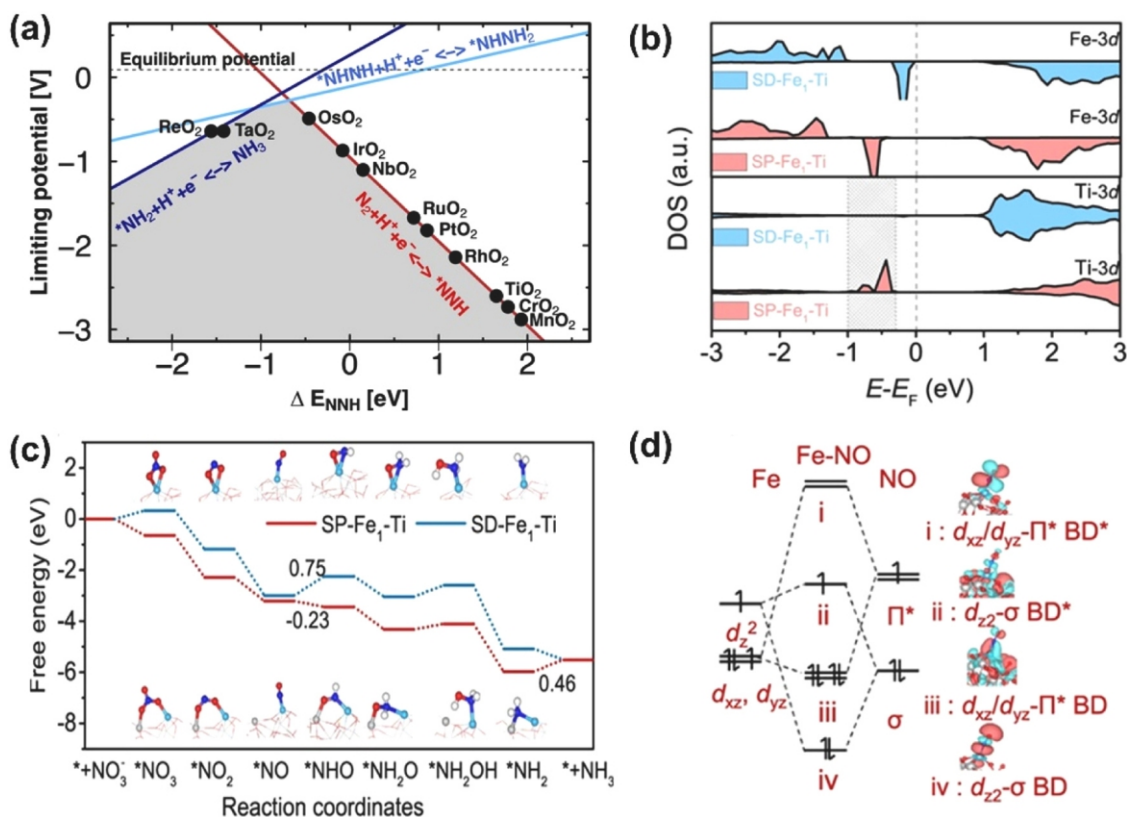


Fig. 3. (a) The scaling relationships for electrochemical ammonia formation on transition metal oxides. (b) Density of states Fe and Ti on SD-Fe<sub>1</sub>-Ti and SP-Fe<sub>1</sub>-Ti. (c) Calculated free energy diagrams for NITRR on SD-Fe<sub>1</sub>-Ti and SP-Fe<sub>1</sub>-Ti. (d) The diagrams of Fe atom orbitals and NO molecules orbitals interactions.

(a) Reproduced with permission from ref. [27]. Copyright 2017, ACS Publications. (b-d) Reproduced with permission from ref. [30]. Copyright 2024, Springer Nature.

demonstrate that catalysts with the appropriate adsorption capacity are located in the upper region of the volcano curves. In 1999, the Brønsted-Evans-Polanyi (BEP) relationship was reported in the heterogeneous catalytic system [26]. The scaling relationship constraints between different reaction intermediates are one reason for the limited reaction rate. As presented in Fig. 3a, ReO<sub>2</sub> and TaO<sub>2</sub> were selected as the possible ammonia synthesis catalysts. Although OsO<sub>2</sub> had a lower overpotential for ammonia synthesis, the strong proton adsorption than  $^*\text{NNH}$  on the surface was detrimental to the first protonic step of N<sub>2</sub> ( $\text{N}_2 + \text{H}^+ + e^- \rightarrow ^*\text{NNH}$ ) [27]. These inherent scaling relationships largely affect the design of efficient nitrogen reduction catalysts [28]. To overcome this limitation, modification of the active sites with the function to distinguish different N intermediates and transition state structures is highly demanded. Apart from the intrinsic catalytic reactivity, high proton and electron conductivity are also critical for the rapid and selective protonation of nitrogen intermediates to ammonia.

Besides, the utilization of NO<sub>x</sub> as the N resource with a low activation energy other than inert nitrogen molecules would be one available alternative for the highly active and selective ammonia synthesis [29]. Recently, Zhang and coworkers reported spin-polarized Fe<sub>1</sub>-Ti pairs sites could realize a high electroreduction nitrate to ammonia yield rate  $4.44 \times 10^{-6} \text{ mol mg}_{\text{Fe}}^{-1} \text{ s}^{-1}$  with a high FE of 95.2% via NO<sub>3</sub><sup>-</sup> reduction [30]. The spin-polarized Fe<sub>1</sub> provided the spin electrons to promote the deoxygenation of NO<sub>3</sub><sup>-</sup> to  $^*\text{NO}$  and the hydrogenation of  $^*\text{NO}$  to  $^*\text{NHO}$ . Meanwhile, spin-polarized Ti promoted the electron transfer from oxygen vacancies to  $d_{z^2}$  orbitals of Ti and then to the  $^*\text{NHO}$  (Figs. 3b–d). Thus, the rational design of electrocatalysts to modulate the NO<sub>x</sub> adsorption and accelerate the electron/proton transfer process would be conducive to boosting efficient ammonia production.

Furthermore, stable catalytic structures with high tolerance to water, carbon and sulfur impurities are required. Generally, changes in catalytic structures under high voltage or high temperature and blockage of the active sites by impurities are the main reasons for the performance degradation. A variety of methods, such as high valence metal doping (Ta, Nb, Mo, etc.), robust support interaction, modulation of the coking and sulfur tolerance, etc. have been developed to tackle the unrecoverable performance degradation [31].

### 3. PCECs in electrochemical ammonia synthesis

#### 3.1. Cell configurations

As shown in Fig. 4, two types of PCECs have been developed for ammonia synthesis, such as single-chamber and dual-chamber reactors. The single-chamber reactor is similar to the conventional Haber-Bosch fixed bed reactor, where H<sub>2</sub> and N<sub>2</sub> are mixed as the feed gases in a single chamber. The main difference from the Haber-Bosch process is that the voltage is applied to both sides of the cell. Driven by electricity, more protons are pumped from the anode electrode to the cathode, leading to the enhancement of catalytic activity. The process is known as the non-Faradaic electrochemical modification of catalytic activity (NEMCA) [32]. The NEMCA effect can be evaluated by the enhancement factor ( $\Lambda$ ) which is defined as:

$$\Lambda = \Delta r(I/2F)^{-1}$$

Where  $\Delta r$  is the difference in reaction rates between with and without applied voltage,  $I$  is the current density with applied voltage,  $F$  is Faraday's constant ( $96,485 \text{ C mol}^{-1}$ ).  $I/2F$  is the proton transport rate through the electrolyte from the anode to the cathode. when the value of  $\Lambda > 1$ , the NEMCA effect is happens [24].

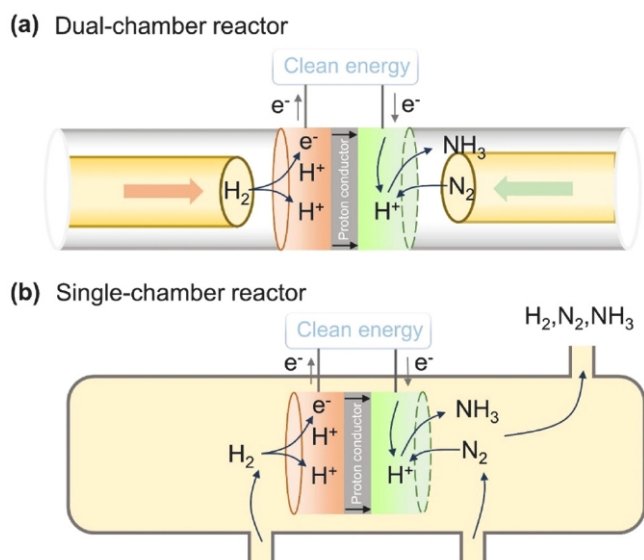


Fig. 4. Schematic illustration of PCECs configurations. (a) Dual-chamber configuration and (b) single-chamber configuration.

However, this phenomenon is only apparent when the NRR has not reached the thermodynamic equilibrium, which means that the single chamber reactors are still constrained by the thermodynamic equilibrium like the HB process. Moe Okazaki and Junichiro Otomo investigated three different Fe-based electrode structures in single-chamber reactors: a metal (Fe), a cermet (Fe + BaZr<sub>0.8</sub>Y<sub>0.2</sub>O<sub>3-δ</sub>), and a mixed ionic-electronic conductor (BaZr<sub>0.5</sub>Fe<sub>0.4</sub>Y<sub>0.1</sub>O<sub>3-δ</sub>). It was found the electrochemical promotion mainly occurred near the interface between electrolytes and electrodes or the triple phase boundaries because of sufficient proton supply [33]. The rate of ammonia synthesis is also contingent upon the cathodic polarization. The reduction of ohmic resistance in single cells can facilitate the application of sufficient polarization at the cathode, thereby promoting the ammonia synthesis rates [34].

The dual-chamber configuration is one of the most widely and deeply developed ammonia synthesis reactors. In this reactor, H<sub>2</sub> and N<sub>2</sub> as the feed gases are directly delivered to the anode and the cathode, respectively. The applied voltage determines the operating current density, which is closely related to the FE and the rate of ammonia synthesis. The volcanic relationship between the ammonia synthesis rate and the current density suggests that the maximum rate can only be reached at the intermediate current density. While FE decreases continuously with the increasing current density due to the favorable hydrogen evolution reaction (HER) and potential electron leakage [35]. Compared to the conventional HB process, the dual-chamber reactors can overcome the thermodynamic constraints by directly converting electrical energy into chemical energy, contributing to a higher ammonia conversion rate at ambient pressure.

### 3.2. Typical cathodes

In PCECs system, the eNRR to ammonia occurs at the cathode and protons are produced at the anode by hydrogen oxidation, vapor methane reforming, or water decomposition process, and then transported to the cathode via a proton-conducting electrolyte membrane. Over recent years, various electrocatalytic electrodes, including noble metals or oxides, perovskite oxides, etc. have been established. Extensive attention is attached to creating surface active sites and improving the mixed electron and proton conductivity of the materials.

#### 3.2.1. Engaging noble metal sites

Nowadays, noble metal (Ag-Pd) is one of the most widely used eNRR electrode materials with an ammonia synthesis rate of

$\sim 10^{-9} \text{ mol s}^{-1} \text{ cm}^{-2}$  at 500–650 °C [36,37]. When the operating temperature is decreased, the ammonia synthesis rates will be reduced [38–42]. In the molten salt systems (100–500 °C), it can reach around  $10^{-9} \text{ mol s}^{-1} \text{ cm}^{-2}$  while the achieved ammonia synthesis rates in most ambient ammonia systems (<100 °C) are generally below  $10^{-9} \text{ mol s}^{-1} \text{ cm}^{-2}$ . Pd enables sufficient proton transport and enhances the adsorption of nitrogen molecules, while Ag improves the electrode conductivity for rapid electron transfer [43]. In contrast, the ammonia synthesis rate of Pt is two orders of magnitude lower, probably due to the excellent HER activity of Pt [44]. It has been widely reported that the noble metal and transition metal oxides composite catalysts enhance both activity and stability. La<sub>0.5</sub>Sr<sub>0.5</sub>Ti<sub>0.6</sub>Ru<sub>0.4</sub>O<sub>3-δ</sub> with *in-situ* high dispersion Ru-nanoparticles on the surface exhibited a higher selectivity than the conventional Ag-Pd catalyst [45,46]. *In-situ* Ru nanoparticles on the surface of the mixed protonic-electronic conduction BaCe<sub>0.9-x</sub>Y<sub>0.1</sub>Ru<sub>x</sub>O<sub>3-δ</sub> electrode exhibited a higher ammonia formation rate ( $1 \times 10^{-11} \text{ mol s}^{-1} \text{ cm}^{-2}$ ) than the Ru-doped LaSr<sub>1-x</sub>Ti<sub>x</sub>O<sub>3-δ</sub> ( $3.8 \times 10^{-12} \text{ mol s}^{-1} \text{ cm}^{-2}$ ) through promoting the protons transport to the Ru surface [47]. Recently, Ding's group designed PrBa<sub>0.5</sub>Sr<sub>0.5</sub>CoFeO<sub>5+δ</sub>-Ru/La<sub>0.25</sub>Ce<sub>0.75</sub>O<sub>2-δ</sub> (P/LDCRu-W, LDC: lanthanum-doped cerium dioxide.) multi-composite catalyst by post-synthesized hydrothermal and impregnation treatments (Fig. 5a) [48]. As shown in Figs. 5b and c, the ammonia synthesis was tested with different applied voltage, the electrode of P/LDCRu-W exhibited a high partial current densities and ammonia synthesis rate ( $8.11 \times 10^{-8} \text{ mol s}^{-1} \text{ cm}^{-2}$  at 400 °C), which is up to 100-fold higher than the current state-of-the-art electrolyzers. The excellent catalytic activity (Ru5 > Ru1 > Ru14) could be attributed to the interplay between the *in-situ* generated Ru clusters with an optimized size of Ru particle and the *in-situ* formed Ce<sup>3+</sup>-OH sites. Density functional theory (DFT) calculations revealed that the surface hydroxylated LDC (LDC-W) with an appropriate loading of Ru could significantly reduce the reaction energy barriers for both N<sub>2</sub> adsorption and the subsequent protonation process. All three hydroxylated LDC-W (H<sub>2</sub>O\_Ru1, H<sub>2</sub>O\_Ru5, H<sub>2</sub>O\_Ru14) had a lower barrier for nitrogen adsorption compared with the pristine LDC (Ru5). Moreover, this catalyst also displayed excellent stability without much performance decay when the cell was operated at 400 °C under H<sub>2</sub>/N<sub>2</sub> atmosphere for 550 h. The synergistic interactions among diverse active sites on multisite catalysts represent a promising strategy for the design of high-performance eNRR electrodes.

#### 3.2.2. Constructing transitional metal sites

The high cost of noble metals significantly blocked their large-scale utilization in ammonia synthesis. Hence, the development of a high abundance, cost-effective eNRR catalyst is paramount to render the commercial implementation of PCECs systems, necessitating extensive efforts in the exploration of noble metal-free electrocatalysts. Perovskite materials have garnered significant attention due to their adaptability of chemical composition, crystal and electronic structure, stability, and adjustable catalytic activity [49]. As reported by Chen and coworkers, Cu-doped LaFeO<sub>3</sub> (LaCu<sub>0.1</sub>Fe<sub>0.9</sub>O<sub>3-δ</sub>) was utilized as the eNRR electrocatalyst, which showed an ammonia synthesis rate of  $5.12 \times 10^{-9} \text{ mol s}^{-1} \text{ cm}^{-2}$  at 650 °C [50]. The synergistic effect between Cu and Fe was the origin of higher NRR activity compared to the parent LaFeO<sub>3-δ</sub>: i) Faster electron transfer through the Fe-O-Cu chain promoted the electron conductivity; ii) Fe<sup>4+</sup>, Cu<sup>+</sup> and oxygen vacancies were all as the electron-deficient species to enhance the activation of the adsorbed nitrogen molecules. Besides, Shao's group reported that the abundant oxygen vacancies and the high content of doping metal (e.g. Ti<sup>3+</sup>) into the perovskite oxide could promote nitrogen decomposition and enhance NRR activity. The developed A-site deficient Sr<sub>0.9</sub>Ti<sub>0.6</sub>Fe<sub>0.4</sub>O<sub>3-δ</sub> afforded a high ammonia synthesis rate ( $6.84 \times 10^{-9} \text{ mol s}^{-1} \text{ cm}^{-2}$  at 650 °C), which was comparable with noble metals [51].

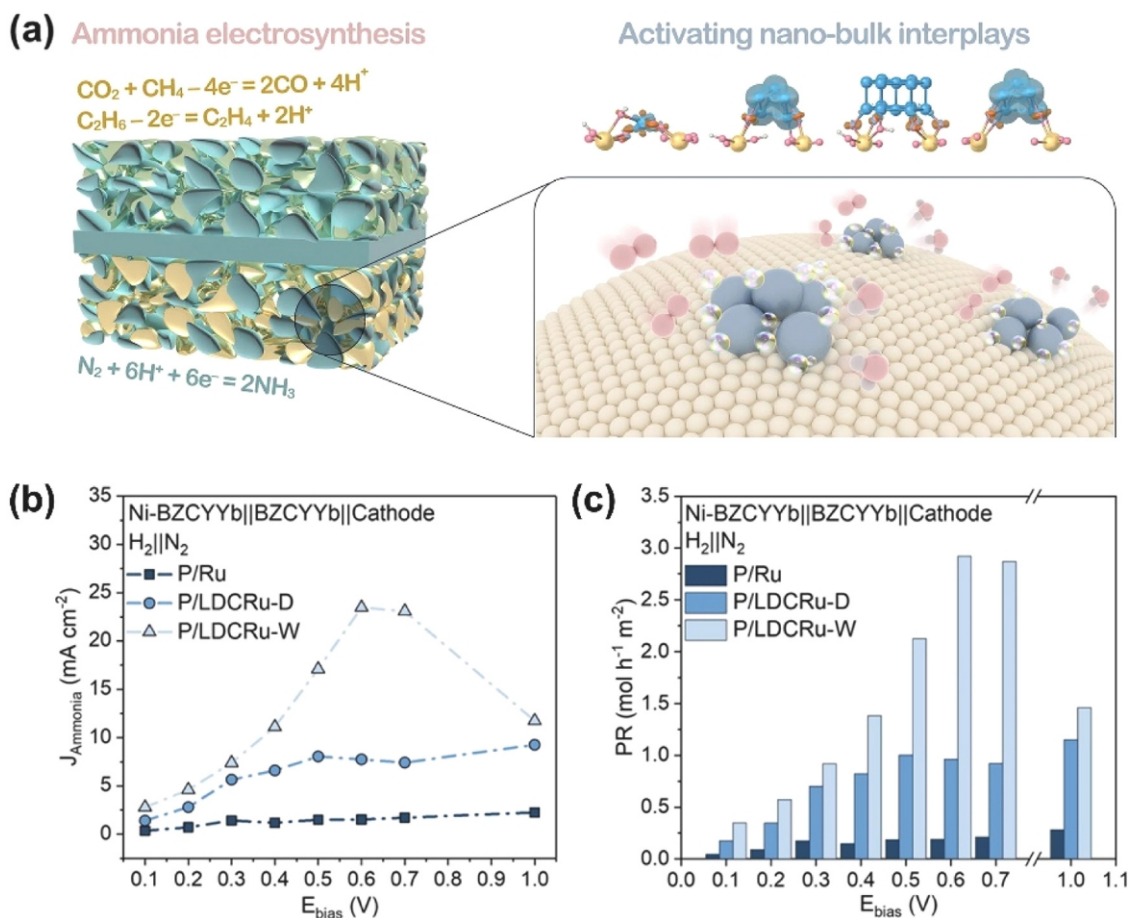


**Fig. 5.** (a) Illustration of PCECs operating module. (b) Partial current densities with different cathodes of eNRR at different  $E_{\text{bias}}$ . (c) Ammonia synthesis with different cathodes of eNRR at different  $E_{\text{bias}}$ .

Reproduced with permission from ref. [48]. Copyright 2022, Elsevier.

### 3.2.3. Introducing lattice nitrogen sites

Given the inherently linear relationship of reactants/intermediates in the traditional adsorbate evolution mechanism (AEM) on the majority of catalysts, it is constrained to further improve their catalytic performance. In this context, the search for catalysts that undergo the reaction pathway of the MvK mechanism would be one appealing choice. In recent studies, transition metal nitrides have been investigated for eNRR via the MvK mechanism by virtue of their abundant lattice nitrogen.

For instance, the lattice nitrogen-participated mechanism on the anti-perovskite nitrides was recently investigated by Zou's group by using high-throughput calculations (Fig. 6a) [52]. The degree of M-N bond strength in the anti-perovskite nitride was proposed as a suitable descriptor for the catalytic activity and structural stability of the nitrogen lattice.  $\text{AgBa}_3\text{N}$ ,  $\text{AlBa}_3\text{N}$ , and  $\text{GaBa}_3\text{N}$  catalysts were predicted as potential NRR electrocatalysts with higher activity and selectivity than the noble metal Ru (Fig. 6b). The high energy barrier steps were mainly the second and third protonation processes of nitrogen species ( $\text{NH} \rightarrow \text{NH}_2$ ,  $\text{NH}_2 \rightarrow \text{NH}_3$ ). A lower overpotential for NRR over these candidates is due to the enhanced adsorption of protons on the lattice nitrogen for favorable NRR and the hindered combination of protons into hydrogen toward the reduction of HER activity. Through investigating the density of initial and steady-state active sites of the oxygen-modified vanadium nitride ( $\text{VN}_{0.75}\text{O}_{0.45}$ ) by isotope quantification experiments, Xu et al. proved that less than 5% of the lattice nitrogen sites could participate in the isotope exchange reaction. The DFT calculation and experiment results indicated that the first protonation step of the adsorbed nitrogen on N vacancies ( $^*\text{N}_2 + 1/2\text{H}_2(\text{g}) \rightarrow ^*\text{N}_2\text{H}$ ) is the potential rate determine step rather than the adsorption of nitrogen

[53]. Ozkan et al. reported that  $\text{Co}_3\text{Mo}_3\text{N}$  could also facilitate the formation of N-H bonds, thereby increasing the synthesis rate of ammonia (Fig. 7a) [54]. Stoukides et al. used VN-Fe composite as the nitrogen reduction catalyst in PCECs and realized an ammonia synthesis rate with a maximum value of  $1.89 \times 10^{-9} \text{ mol s}^{-1} \text{ cm}^{-2}$  at 600 °C and an ammonia FE of 5.5% (Figs. 7b and c) [35]. The  $\text{Mn}_4\text{N}$  also exhibited a similar ammonia synthesis rate via the hydrogenation of lattice nitrogen during the power generation process in the solid oxide fuel cells [55]. However, there remain critical challenges regarding the instability of the metal nitrides under high-temperature conditions. Duncan et al. found the  $\text{NbN}_x\text{O}_y$  decomposed into an  $\text{Nb}_2\text{O}_5$  phase under an  $\text{N}_2$  atmosphere at elevated temperatures [56]. Currently, the design of metal nitride catalysts relies primarily on a trial-and-error approach, which is time-consuming and economically burdensome.

### 3.3. Representative electrolytes

The ammonia synthesis by  $\text{N}_2$  and  $\text{H}_2$  is a typical exothermic reaction, and it is more favorable at a low temperature. Nowadays, the operating temperature of the PCECs is mainly above 500 °C, which will primarily restrict the advancement of ammonia synthesis technology. The main reasons are included: i) the favorable ammonia decomposition at high temperatures compared with the ammonia synthesis reaction; ii) the higher demands on the electrode materials and the related operating equipment at high operating temperatures. For example, the possible diffusion of chromium oxide ( $\text{CrO}$ ,  $\text{CrO}_2$ ,  $\text{CrO}_3$ ) of the common ferritic steel interconnect materials into the interconnect and cathode will lead to poisoning of the electrodes at elevated temperatures, especially under the humid atmosphere [57–59]. Yoo and coworkers

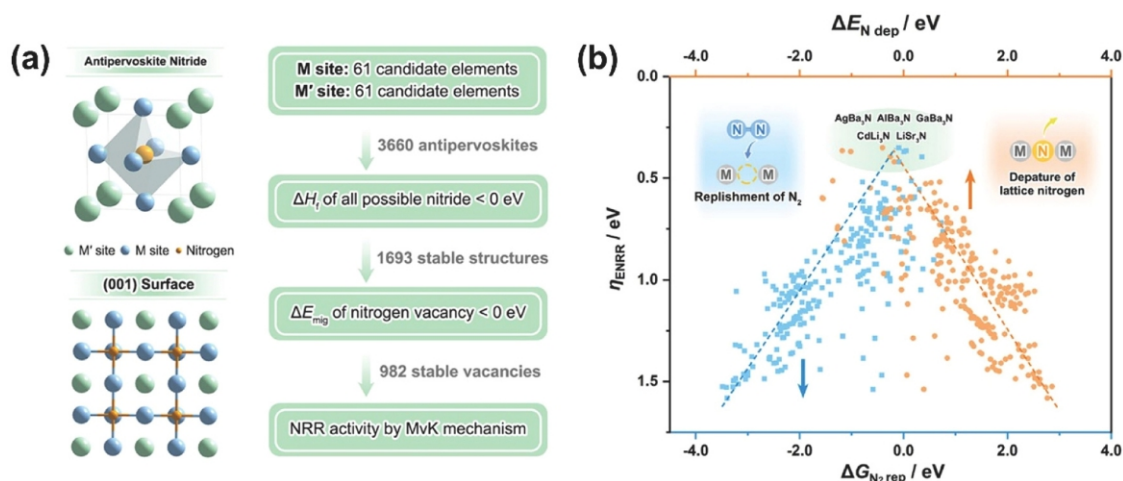


**Fig. 6.** (a) The crystal structure of anti-perovskite and the steps of high throughput calculations. (b) Volcanic curves between  $\Delta E_{\text{N dep}}$  and  $\Delta G_{\text{rds}}$ . Reproduced with permission from ref. [52]. Copyright 2023, Wiley Online Library.

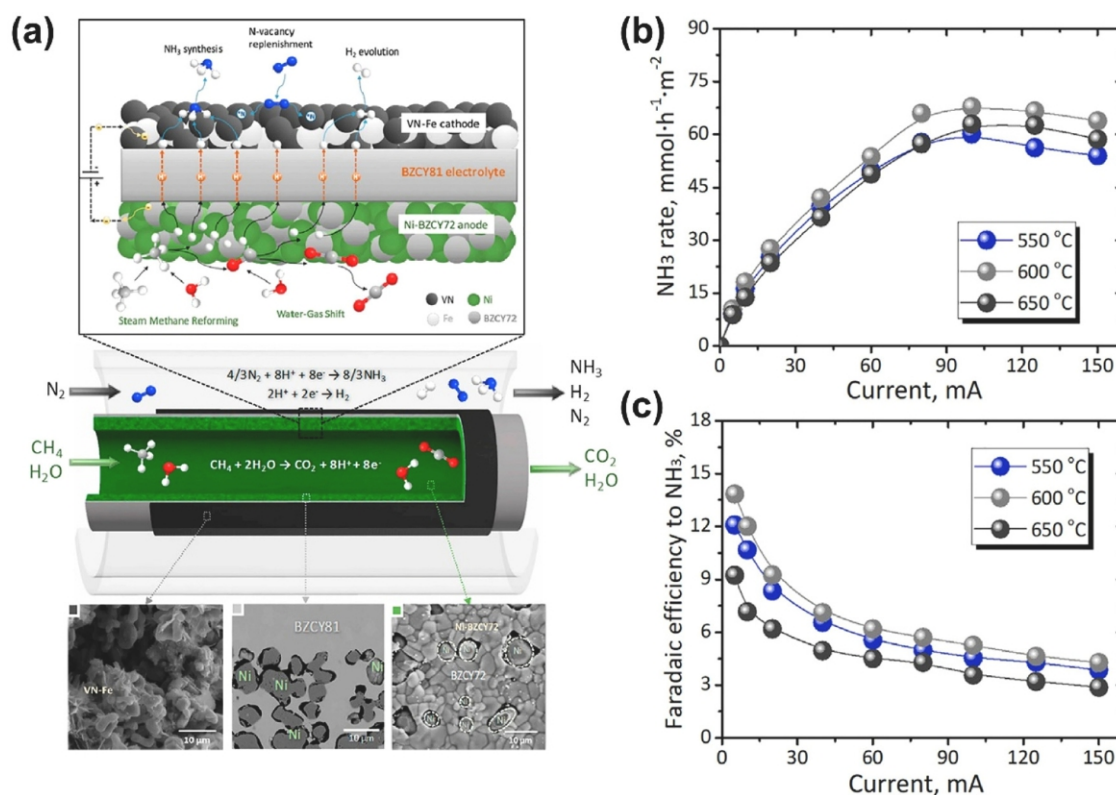


**Fig. 7.** (a) Schematic illustration of the tubular PCECs for ammonia synthesis. (b) and (c) Ammonia synthesis rates and FE at different current densities. Reproduced with permission from ref. [35]. Copyright 2020, Elsevier.

investigated the relationship between proton conductivity and ammonia synthesis using the bimetallic Ag-Pd cathode as a model electrocatalyst, and summarized an empirical equation using the power-law relationship [60]:

$$\log r_{\text{NH}_3} = a + b \log(\sigma_{\text{H}^+} T)$$

The high proton conductivity and low electronic conductivity are key factors for the ideal electrolytes of PCECs to realize ammonia synthesis at lower reaction temperatures [8].

In 1998, Marnellos and Stoukides used SrCe<sub>0.95</sub>Yb<sub>0.05</sub>O<sub>3</sub> as the proton conductor for the electrochemical ammonia synthesis [61]. The Pd was used as the electrode on both sides of SrCe<sub>0.95</sub>Yb<sub>0.05</sub>O<sub>3</sub> to form a sandwich configuration (Pd||SrCe<sub>0.95</sub>Yb<sub>0.05</sub>O<sub>3-δ</sub>||Pd). The ammonia

synthesis rate reached 10<sup>-9</sup> mol s<sup>-1</sup> cm<sup>-2</sup> at 570 °C and more than 78% of the electrochemically supplied hydrogen was converted to ammonia. To date, the acceptor-doped barium cerates and barium zirconates are the most widely studied proton-conducting electrolytes [62–64]. Unfortunately, doped barium zirconates suffer from poor sinter ability, and thereby high grain boundary resistance, which severely limits the operation at low temperatures [65]. Although acceptor-doped barium ceramics exhibit high ionic conductivity, their poor chemical stability against common contaminants such as H<sub>2</sub>O and CO<sub>2</sub> poses a grand challenge for long-term durability [66].

In order to improve the chemical stability of the electrolyte, the donor doping strategy can be an effective approach. Recently, Liu's group has developed a series of H<sub>2</sub>O and CO<sub>2</sub> tolerant electrolytes

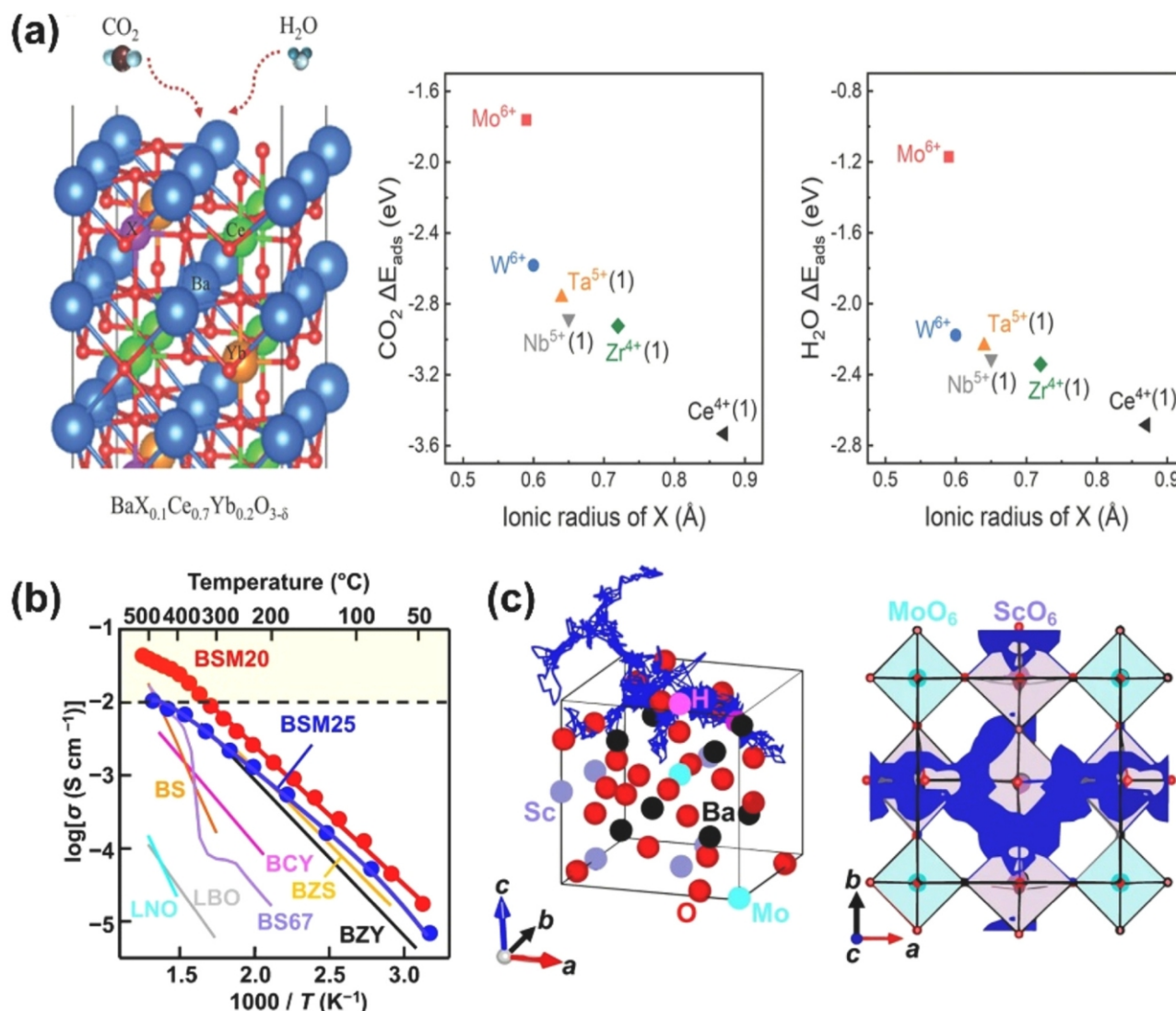


**Fig. 8.** (a) The diagram of  $\text{H}_2\text{O}$  and  $\text{CO}_2$  react with  $\text{BaX}_{0.1}\text{Ce}_{0.7}\text{Yb}_{0.2}\text{O}_{3-\delta}$  and relevant reaction energy of different metal ions. (b) Arrhenius of bulk conductivity of different electrolytes. (c) The simulated proton migration pathways in the bulk lattice of  $\text{Ba}_8\text{Sc}_6\text{Mo}_2\text{O}_{23}$  ( $\text{H}_2\text{O}$ ).

(a) Reproduced with permission from ref. [68]. Copyright 2023, Wiley Online Library. (b) Reproduced with permission from ref. [69]. Copyright 2023, Springer Nature.

$\text{BaM}_x\text{Ce}_y\text{Yb}_{1-x-y}\text{O}_{3-\delta}$  ( $M = \text{Nb}, \text{Ta}, \text{Mo}, \text{W}$ ) [67,68]. As presented in Fig. 8a, the high valence ions  $M$  substituting  $\text{Ce}$  with  $\text{Zr}$  improved the reaction energy ( $E_{\text{ads}}$ ) of electrolytes with  $\text{H}_2\text{O}$  and  $\text{CO}_2$  and exhibited excellent tolerance to the impurities. Normally, the donor-doped materials possess lower proton conductivity due to the decrease in the oxygen vacancy content. The regulation of the ionic stoichiometry can bring a relatively high conductivity to these perovskite electrolytes, where two extra  $\text{Yb}$  atoms are needed to maintain the oxygen vacancy concentration when a six-valence ion ( $\text{Mo}, \text{W}$ ) is introduced into the B sites. Upon this strategy, various low-temperature electrolyte materials have been developed. Yashima and coworkers have proposed an electrolyte  $\text{BaSc}_{0.8}\text{Mo}_{0.2}\text{O}_{2.8}$  with abundant intrinsic oxygen vacancies [69].  $\text{Mo}$  doped  $\text{BaScO}_{2.5}$  (Fig. 8b) exhibited high proton conductivity (e.g.,  $0.01 \text{ S cm}^{-1}$  at  $320^\circ\text{C}$ ) and high chemical stability under oxidizing, reducing and  $\text{CO}_2$  atmospheres. The weaker proton trapping was responsible for the excellent proton conductivity because of the repulsion between the donor  $\text{Mo}_{\text{Sc}}^{6+}$  and  $\text{H}^+$  in the lattice (Fig. 8c). Recently, Wang et al. reported an excellent  $\text{CO}_2$ -tolerant  $\text{La}_{5.5}\text{WO}_{11.25-\delta}$  (LWO) membrane reactor (Figs. 9a and b), which achieved a high FE of 43.8% with

an ammonia rate of  $3.78 \times 10^{-9} \text{ mol s}^{-1} \text{ cm}^{-2}$  at  $350^\circ\text{C}$  and successfully operated for 100 h without much degradation [70]. As presented in Figs. 9c and d, the LWO exhibited superior stability to  $\text{CO}_2$  compared with other widely used electrolyte materials. The highly activated protons from the fuel electrode side of the LWO electrolyte membrane promoted the protonation process of nitrogen-containing intermediates. As a result, the rate-determining step was changed from the protonation process to the  $\text{N}_2$  activation on the Ru surface, with the increased utilization of protons limiting HER and enhancing ammonia FE. Recently,  $\text{La}_2\text{Ce}_2\text{O}_7$  (LCO) based electrolyte materials have been proposed because of their high ionic conductivity and high chemical stability. While serious electronic leakage of LCO because of the reduction of  $\text{Ce}^{4+}$  to  $\text{Ce}^{3+}$  under a reducing environment is a serious issue that needs to be addressed. Besides, the protonic conductivity is relatively low compared to current proton conductors and needs to be further improved [71,72]. To facilitate the development of ammonia reactors, extensive efforts should be dedicated to exploring the proton conductor electrolyte that can be operated at lower operating temperatures.

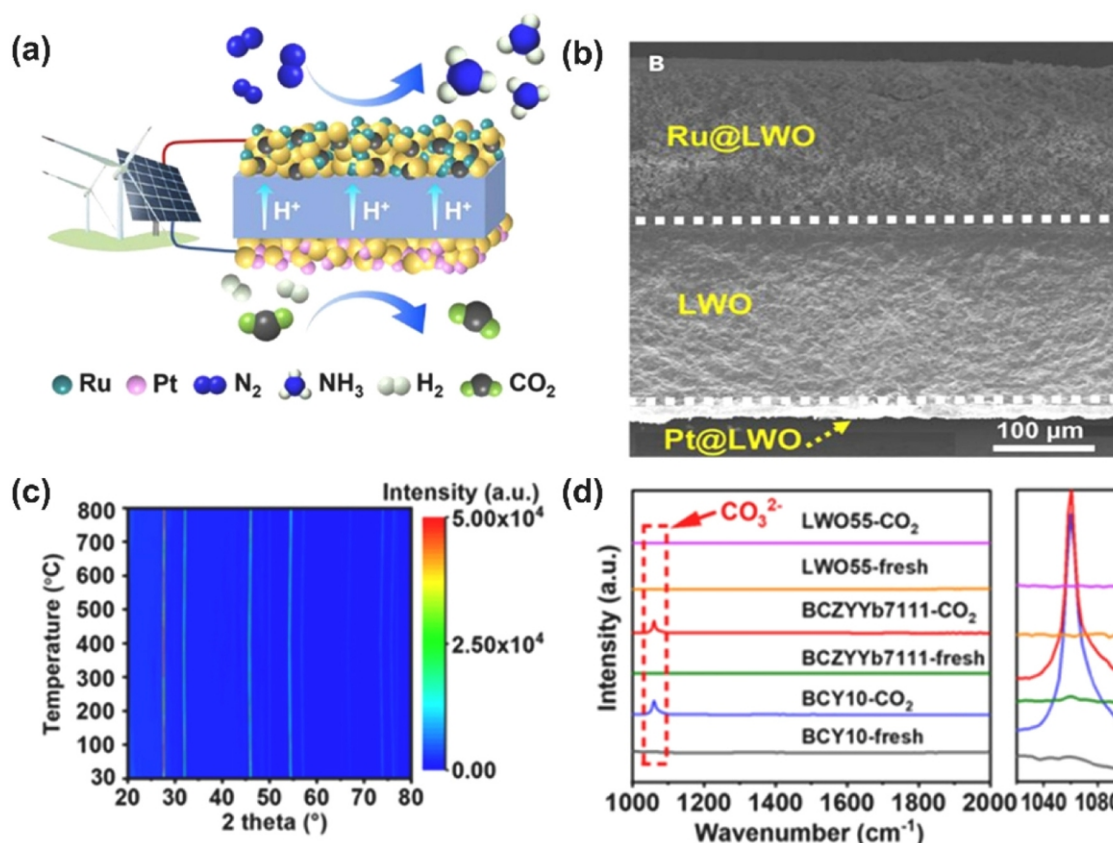


**Fig. 9.** (a) The illustration of LWO protonic ceramic membrane reactor. (b) Cross-section SEM image of the LWO protonic ceramic membrane reactor. (c) *In-situ* XRD patterns of LWO from 30 to 800 °C under CO<sub>2</sub> atmosphere. (d) Raman spectra of widely used proton-conducting electrolyte materials and LWO were obtained after exposure to a CO<sub>2</sub> atmosphere at 500 °C for 100 h.

Reproduced with permission from ref. [70]. Copyright 2023, Elsevier.

#### 4. Conclusion and perspective

Overall, PCECs with the ability to activate nitrogen molecules under atmospheric conditions have exhibited great potential for the distributed commercial production of green ammonia. In this review, we have provided a summary of the eNRR mechanism and the recent advances in electrolyte and electrode materials of PCECs for electrochemical ammonia synthesis. Despite many opportunities, the key components of PCECs and the stack remain a major challenge in advancing commercial implementation. Prospects for the future development of PCECs in ammonia synthesis are highlighted below:

##### 4.1. Insightful understanding of the reaction process

It is important to import various characterization tools to monitor the dynamic changes of the electrode and the adsorption/desorption of intermediates. An insightful analysis of the reaction process and the factors affecting the performance of PCECs can be performed. Thus far, mechanistic studies of the electrochemical ammonia synthesis reaction in PCECs are extremely difficult and limited by the characterization techniques at high temperatures. Thus, the advancement of the *in-situ* characterization techniques (e.g., *in-situ* X-ray Diffraction technique, synchrotron X-ray Absorption Spectroscopy, Raman, Fourier Transform Infrared spectroscopy, Transmission Electron Microscopy) is helpful to understand the catalytic process for the future rational design of effective materials.

##### 4.2. Rational design of electrodes and electrolytes

At present, the ammonia synthesis rate of PCECs is generally  $10^{-8} \sim 10^{-9} \text{ mol s}^{-1} \text{ cm}^{-2}$  with a low FE (<10%), which is lower

than the commercially viable target ( $> 9.3 \times 10^{-7} \text{ mol s}^{-1} \text{ cm}^{-2}$ ) [73]. Hence, the development of novel mixed ionic and electronic conductors with high ammonia synthesis rates remains a top priority at intermediate temperatures ( $\sim 400 \text{ }^\circ\text{C}$  or less). Both the composition and the topological structure of the catalysts are key factors influencing the activity of the ammonia synthesis. Advances in the characterization and theoretical studies offer great opportunities for the reaction-oriented design of advanced materials, particularly based on data-driven techniques. In addition, NO<sub>x</sub> can be used as a nitrogen resource instead of nitrogen molecules due to its low bonding N-O energy for the highly active and selective ammonia synthesis, where the catalytic electrode should be highly stable under the NO<sub>x</sub> atmosphere. What's more, attention should be attached to the electrolyte with high proton conductivity and inhibited electron migration, which can supply sufficient proton resources to facilitate the hydrogenation step of active nitrogen to ammonia.

##### 4.3. Effective strategies for long-term stability

Long-term stability under high temperatures places higher demands on the whole system of PCECs, including the intrinsic stability of the electrode and electrolyte, the interface, etc. In addition to improving the intrinsic stability of the materials, it is pointed out that the well-matching of each component is also pivotal to stabilizing the interface of the device. For instance, the matched thermal expansion coefficient (TEC) of the electrodes and electrolytes will bring similar thermal stress to the electrolyte-electrode interface and contribute to the long-term durability of PCECs.

#### 4.4. Beyond the laboratory to the practical application

Currently, ammonia synthesis experiments are mainly based on small-scale laboratory equipment, which is different from large-scale industrialization. To improve the availability and affordability of PCECs for practical ammonia production, the optimization of cell configuration, stack assembly engineering, and operating parameters should be carried out.

#### Author contributions

The manuscript was written through contributions of all authors. All authors have given approval to the final version of the manuscript.

#### Declaration of Competing Interest

The authors declare no competing interests.

#### Acknowledgments

This work was supported by the National Key R&D Program of China (2022YFB4002601), the National Natural Science Foundation of China (52273277, 52072362 and 52302119), Jilin Province Science and Technology Development Plan Funding Project (SKL202302039 and 20230201150GX) and Youth Innovation Promotion Association CAS (2021223). H.-X. Zhong acknowledges funding from the National Natural Science Foundation of China Outstanding Youth Science Foundation of China (Overseas).

#### References

- [1] A. Wojcik, H. Middleton, I. Damopoulos, J. Van herle, Ammonia as a fuel in solid oxide fuel cells, *J. Power Sources* 118 (2003) 342.
- [2] W.I. David, J.W. Makepeace, S.K. Callear, H.M. Hunter, J.D. Taylor, T.J. Wood, M.O. Jones, Hydrogen production from ammonia using sodium amide, *J. Am. Chem. Soc.* 136 (2014) 13082.
- [3] Y. Li, H.S. Pillai, T. Wang, S. Hwang, Y. Zhao, Z. Qiao, Q. Mu, S. Karakalos, M. Chen, J. Yang, et al., High-performance ammonia oxidation catalysts for anion-exchange membrane direct ammonia fuel cells, *Energy Environ. Sci.* 14 (2021) 1449.
- [4] H. Liu, Ammonia synthesis catalyst 100 years: practice, enlightenment and challenge, *Chin. J. Catal.* 35 (2014) 1619.
- [5] D. Ye, S.C.E. Tsang, Prospects and challenges of green ammonia synthesis, *Nat. Synth.* 2 (2023) 612.
- [6] H. Shen, C. Choi, J. Masa, X. Li, J. Qiu, Y. Jung, Z. Sun, Electrochemical ammonia synthesis: mechanistic understanding and catalyst design, *Chem* 7 (2021) 1708.
- [7] C. Guo, J. Ran, A. Vasileff, S.-Z. Qiao, Rational design of electrocatalysts and photo (electro)catalysts for nitrogen reduction to ammonia (NH<sub>3</sub>) under ambient conditions, *Energy Environ. Sci.* 11 (2018) 45.
- [8] C. Duan, R. Kee, H. Zhu, N. Sullivan, L. Zhu, L. Bian, D. Jennings, R. O'Hayre, Highly efficient reversible protonic ceramic electrochemical cells for power generation and fuel production, *Nat. Energy* 4 (2019) 230.
- [9] M. Saqib, I.-G. Choi, H. Bae, K. Park, J.-S. Shin, Y.-D. Kim, J.-I. Lee, M. Jo, Y.-C. Kim, K.-S. Lee, et al., Transition from perovskite to misfit-layered structure materials: a highly oxygen deficient and stable oxygen electrode catalyst, *Energy Environ. Sci.* 14 (2021) 2472.
- [10] W. Wu, L.-C. Wang, H. Hu, W. Bian, J.Y. Gomez, C.J. Orme, H. Ding, Y. Dong, T. He, J. Li, D. Ding, Electrochemically engineered, highly energy-efficient conversion of ethane to ethylene and hydrogen below 550 °C in a protonic ceramic electrochemical cell, *ACS Catal.* 11 (2021) 12194.
- [11] F. He, Y. Zhou, T. Hu, Y. Xu, M. Hou, F. Zhu, D. Liu, H. Zhang, K. Xu, M. Liu, Y. Chen, An efficient high-entropy perovskite-type air electrode for reversible oxygen reduction and water splitting in protonic ceramic cells, *Adv. Mater.* 35 (2023) e2209469.
- [12] F. Liu, H. Deng, D. Diercks, P. Kumar, M.H.A. Jabbar, C. Gumeci, Y. Furuya, N. Dale, T. Oku, M. Usuda, et al., Lowering the operating temperature of protonic ceramic electrochemical cells to < 450 °C, *Nat. Energy* 8 (2023) 1145.
- [13] T. Hu, F. Zhu, J. Xia, F. He, Z. Du, Y. Zhou, Y. Liu, H. Wang, Y. Chen, *In situ* engineering of a cobalt-free perovskite air electrode enabling efficient reversible oxygen reduction/evolution reactions, *Adv. Funct. Mater.* 33 (2023) 2305567.
- [14] Y. Song, Y. Chen, W. Wang, C. Zhou, Y. Zhong, G. Yang, W. Zhou, M. Liu, Z. Shao, Self-assembled triple-conducting nanocomposite as a superior protonic ceramic fuel cell cathode, *Joule* 3 (2019) 2842.
- [15] S. Back, Y. Jung, On the mechanism of electrochemical ammonia synthesis on the Ru catalyst, *Phys. Chem. Chem. Phys.* 18 (2016) 9161.
- [16] A.L. Garden, E. Skúlason, The mechanism of industrial ammonia synthesis revisited: calculations of the role of the associative mechanism, *J. Phys. Chem. C* 119 (2015) 26554.
- [17] E. Skulason, T. Bligaard, S. Gudmundsdottir, F. Studt, J. Rossmeisl, F. Abild-Pedersen, T. Vegge, H. Jonsson, J.K. Nørskov, A theoretical evaluation of possible transition metal electro-catalysts for N<sub>2</sub> reduction, *Phys. Chem. Chem. Phys.* 14 (2012) 1235.
- [18] T.N. Ye, S.W. Park, Y. Lu, J. Li, M. Sasase, M. Kitano, T. Tada, H. Hosono, Vacancy-enabled N<sub>2</sub> activation for ammonia synthesis on a Ni-loaded catalyst, *Nature* 583 (2020) 391.
- [19] S.M. Hunter, D.H. Gregory, J.S. Hargreaves, M. Richard, D. Duprez, N. Bion, A study of <sup>15</sup>N/<sup>14</sup>N isotopic exchange over cobalt molybdenum nitrides, *ACS Catal.* 3 (2013) 1719.
- [20] Y. Abghoui, A.L. Garden, V.F. Hlynsson, S. Bjorgvinsdottir, H. Olafsdottir, E. Skulason, Enabling electrochemical reduction of nitrogen to ammonia at ambient conditions through rational catalyst design, *Phys. Chem. Chem. Phys.* 17 (2015) 4909.
- [21] Y. Abghoui, A.L. Garden, J.G. Howalt, T. Vegge, E. Skúlason, Electroreduction of N<sub>2</sub> to ammonia at ambient conditions on mononitrides of Zr, Nb, Cr, and V: a DFT guide for experiments, *ACS Catal.* 6 (2015) 635.
- [22] S.Z. Andersen, V. Colic, S. Yang, J.A. Schwalbe, A.C. Nielander, J.M. McEnaney, K. Enemark-Rasmussen, J.G. Baker, A.R. Singh, B.A. Rohr, et al., A rigorous electrochemical ammonia synthesis protocol with quantitative isotope measurements, *Nature* 570 (2019) 504.
- [23] L. Zhou, C.E. Boyd, Comparison of Nessler, phenate, salicylate and ion selective electrode procedures for determination of total ammonia nitrogen in aquaculture, *Aquaculture* 450 (2016) 187.
- [24] G. Qing, R. Ghazfar, S.T. Jackowski, F. Habibzadeh, M.M. Ashtiani, C.P. Chen, M.R. Smith, T.W. Hamann, Recent advances and challenges of electrocatalytic N<sub>2</sub> reduction to ammonia, *Chem. Rev.* 120 (2020) 5437.
- [25] A.J. Martin, S. Mitchell, C. Mondelli, S. Jaydev, J. Pérez-Ramírez, Unifying views on catalyst deactivation, *Nat. Catal.* 5 (2022) 854.
- [26] V. Pallassana, M. Neurock, Electronic factors governing ethylene hydrogenation and dehydrogenation activity of pseudomorphic PdML/Re(0001), PdML/Ru(0001), Pd(111), and PdML/Au(111) surfaces, *J. Catal.* 191 (2000) 301.
- [27] Á.B. Höskuldsson, Y. Abghoui, A.B. Gunnarsdóttir, E. Skúlason, Computational screening of rutile oxides for electrochemical ammonia formation, *ACS Sustain. Chem. Eng.* 5 (2017) 10327.
- [28] A.J. Medford, A. Vojvodic, J.S. Hummelshøj, J. Voss, F. Abild-Pedersen, F. Studt, T. Bligaard, A. Nilsson, J.K. Nørskov, From the sabatier principle to a predictive theory of transition-metal heterogeneous catalysis, *J. Catal.* 328 (2015) 36.
- [29] Y.-i Kwon, S.K. Kim, Y.B. Kim, S.J. Son, G.D. Nam, H.J. Park, W.-C. Cho, H.C. Yoon, J.H. Joo, Nitric oxide utilization for ammonia production using solid electrolysis cell at atmospheric pressure, *ACS Energy Lett.* 6 (2021) 4165.
- [30] J. Dai, Y. Tong, L. Zhao, Z. Hu, C.T. Chen, C.Y. Kuo, G. Zhan, J. Wang, X. Zou, Q. Zheng, et al., Spin polarized Fe<sub>3</sub>-Ti pairs for highly efficient electroreduction nitrate to ammonia, *Nat. Commun.* 15 (2024) 88.
- [31] K. Pei, Y. Zhou, K. Xu, H. Zhang, Y. Ding, B. Zhao, W. Yuan, K. Sasaki, Y. Choi, Y. Chen, M. Liu, Surface restructuring of a perovskite-type air electrode for reversible protonic ceramic electrochemical cells, *Nat. Commun.* 13 (2022) 2207.
- [32] C.G. Yiokari, G.E. Pitselis, D.G. Polydoros, A.D. Katsaounis, C.G. Vayenas, High-pressure electrochemical promotion of ammonia synthesis over an industrial iron catalyst, *J. Phys. Chem. A* 104 (2000) 10600.
- [33] M. Okazaki, J. Otomo, Iron-based electrode structures for ammonia electrosynthesis cells with proton-conducting ceramic electrolytes, *ECS Trans.* 109 (2022) 3.
- [34] M. Okazaki, J. Otomo, Electrode-supported protonic ceramic electrolysis cells for electrochemically promoted ammonia synthesis at intermediate temperatures, *ACS Omega* 8 (2023) 40299.
- [35] V. Kyriakou, I. Garagounis, A. Vourros, E. Vasileiou, M. Stoukides, An electrochemical Haber-Bosch process, *Joule* 4 (2020) 142.
- [36] Y. Xie, Preparation of La<sub>1.9</sub>Ca<sub>0.1</sub>Zr<sub>2</sub>O<sub>6.95</sub> with pyrochlore structure and its application in synthesis of ammonia at atmospheric pressure, *Solid State Ion.* 168 (2004) 117.
- [37] R. Liu, Y. Xie, J. Wang, Z. Li, B. Wang, Synthesis of ammonia at atmospheric pressure with Ce<sub>0.8</sub>M<sub>0.2</sub>O<sub>2.8</sub> (M=La, Y, Gd, Sm) and their proton conduction at intermediate temperature, *Solid State Ion.* 177 (2006) 73.
- [38] H. Cheng, L.X. Ding, G.F. Chen, L. Zhang, J. Xue, H. Wang, Molybdenum carbide nanodots enable efficient electrocatalytic nitrogen fixation under ambient conditions, *Adv. Mater.* 30 (2018) e1803694.
- [39] H. Wang, L. Wang, Q. Wang, S. Ye, W. Sun, Y. Shao, Z. Jiang, Q. Qiao, Y. Zhu, P. Song, et al., Ambient electrosynthesis of ammonia: electrode porosity and composition engineering, *Angew. Chem. Int. Ed.* 57 (2018) 12360.
- [40] B.H.R. Suryanto, D. Wang, L.M. Azofra, M. Harb, L. Cavallo, R. Jalili, D.R.G. Mitchell, M. Chatti, D.R. MacFarlane, MoS<sub>2</sub> polymorphic engineering enhances selectivity in the electrochemical reduction of nitrogen to ammonia, *ACS Energy Lett.* 4 (2018) 430.
- [41] Mi Tsuyoshi, N. Tokujiro, N. Toshiyuki, I. Yasuhiko, Electrolytic synthesis of ammonia in molten salts under atmospheric pressure, *J. Am. Chem. Soc.* 125 (2003) 334.
- [42] Y. Bicer, I. Dincer, Performance assessment of electrochemical ammonia synthesis using photoelectrochemically produced hydrogen, *Int. J. Energy Res.* 41 (2017) 1987.
- [43] B. Wang, T. Li, F. Gong, M.H.D. Othman, R. Xiao, Ammonia as a green energy carrier: electrochemical synthesis and direct ammonia fuel cell - a comprehensive review, *Fuel Process. Technol.* 235 (2022) 107380.
- [44] D.S. Yun, J.H. Joo, J.H. Yu, H.C. Yoon, J.-N. Kim, C.-Y. Yoo, Electrochemical ammonia synthesis from steam and nitrogen using proton conducting yttrium doped barium zirconate electrolyte with silver, platinum, and lanthanum strontium cobalt ferrite electrocatalyst, *J. Power Sources* 284 (2015) 245.

- [45] J. Otomo, N. Noda, F. Kosaka, Electrochemical synthesis of ammonia with proton conducting solid electrolyte fuel cells at Intermediate Temperatures, *ECS Trans.* 68 (2015) 2663.
- [46] F. Kosaka, N. Noda, T. Nakamura, J. Otomo, *In situ* formation of Ru nanoparticles on  $\text{La}_{1-x}\text{Sr}_x\text{TiO}_{3-\delta}$  based mixed conducting electrodes and their application in electrochemical synthesis of ammonia using a proton-conducting solid electrolyte, *J. Mater. Sci.* 52 (2016) 2825.
- [47] F. Kosaka, T. Nakamura, J. Otomo, Electrochemical ammonia synthesis using mixed protonic-electronic conducting cathodes with resolved Ru-nanoparticles in proton conducting electrolysis cells, *J. Electrochem. Soc.* 164 (2017) F1323.
- [48] M. Li, B. Hua, W. Wu, L.-C. Wang, Y. Ding, M.M. Welander, R.A. Walker, D. Ding, Activating nano-bulk interplays for sustainable ammonia electrosynthesis, *Mater. Today* 60 (2022) 31.
- [49] K. Chu, F. Liu, J. Zhu, H. Fu, H. Zhu, Y. Zhu, Y. Zhang, F. Lai, T. Liu, A general strategy to boost electrocatalytic nitrogen reduction on perovskite oxides via the oxygen vacancies derived from a-site deficiency, *Adv. Energy Mater.* 11 (2021) 2003799.
- [50] W. Guo, Y. Li, S.-D. Li, Z. Shao, H. Chen, Ammonia synthesis via a protonic ceramic electrolysis cell (PCEC) using  $\text{LaCu}_{0.1}\text{Fe}_{0.9}\text{O}_{3-\delta}$ , *Catal. J. Mater. Chem. A* 12 (2024) 1200.
- [51] K. Wang, H. Chen, S.-D. Li, Z. Shao,  $\text{Sr}_x\text{Ti}_{0.6}\text{Fe}_{0.4}\text{O}_{3-\delta}$  ( $x = 1.0, 0.9$ ) catalysts for ammonia synthesis via proton-conducting solid oxide electrolysis cells (PCECs), *J. Mater. Chem. A* 10 (2022) 24813.
- [52] M. Zhang, X. Ai, X. Liang, H. Chen, X. Zou, Key role of local chemistry in lattice nitrogen-participated  $\text{N}_2$ -to- $\text{NH}_3$  electrocatalytic cycle over nitrides, *Adv. Funct. Mater.* 33 (2023) 2306358.
- [53] X. Yang, S. Kattel, J. Nash, X. Chang, J.H. Lee, Y. Yan, J.G. Chen, B. Xu, Quantification of active sites and elucidation of the reaction mechanism of the electrochemical nitrogen reduction reaction on vanadium nitride, *Angew. Chem. Int. Ed.* 58 (2019) 13768.
- [54] M. Ferree, S. Gunduz, J. Kim, R. LaRosa, Y. Khalifa, A.C. Co, U.S. Ozkan, Enhanced  $\text{N}_2$  activation on a composite  $\text{Co}_3\text{Mo}_3\text{N}$  nitride and  $\text{La}_{0.6}\text{Sr}_{0.4}\text{Co}_{0.2}\text{Fe}_{0.8}\text{O}_3$  perovskite cathode for high-temperature electrochemical ammonia synthesis, *ACS Sustain. Chem. Eng.* 11 (2023) 5007.
- [55] O. Rahumi, M.K. Rath, A. Kossenko, M. Zinigrad, K. Borodianskiy, Heterogeneous catalyst-modified anode in solid oxide fuel cells for simultaneous ammonia synthesis and energy conversion, *ACS Sustain. Chem. Eng.* 11 (2023) 14081.
- [56] V.C.D. Graça, L.I.V. Holz, A.J.M. Araújo, F.J.A. Loureiro, D.P. Fagg, A novel niobium (oxy)nitride-BaCe<sub>0.7</sub>Zr<sub>0.1</sub>Y<sub>0.2</sub>O<sub>3-δ</sub> composite electrode for proton ceramic membrane reactors (PCMRs), *J. Energy Storage* 68 (2023) 107769.
- [57] J.G. Grolig, J. Froitzheim, J.E. Svensson, Coated stainless steel 441 as interconnect material for solid oxide fuel cells: oxidation performance and chromium evaporation, *J. Power Sources* 248 (2014) 1007.
- [58] H. Kurokawa, C. Jacobson, L. Dejonghe, S. Visco, Chromium vaporization of bare and of coated iron-chromium alloys at 1073 K, *Solid State Ion.* 178 (2007) 287.
- [59] R. Sachitanand, M. Sattari, J.-E. Svensson, J. Froitzheim, Evaluation of the oxidation and Cr evaporation properties of selected FeCr alloys used as SOFC interconnects, *Int. J. Hydrog. Energy* 38 (2013) 15328.
- [60] C.-Y. Yoo, J.H. Park, K. Kim, J.-I. Han, E.-Y. Jeong, C.-H. Jeong, H.C. Yoon, J.-N. Kim, Role of protons in electrochemical ammonia synthesis using solid-state electrolytes, *ACS Sustain. Chem. Eng.* 5 (2017) 7972.
- [61] G. Marnellos, M. Stoukides, Ammonia synthesis at atmospheric pressure, *Science* 282 (1998) 98.
- [62] L. Yang, S. Wang, K. Blinn, M. Liu, Z. Liu, Z. Cheng, M. Liu, Enhanced sulfur and coking tolerance of a mixed ion conductor for SOFCs:  $\text{BaZr}_{0.1}\text{Ce}_{0.7}\text{Y}_{0.2-x}\text{Yb}_x\text{O}_{3-\delta}$ , *Science* 326 (2009) 126.
- [63] C. Zuo, S. Zha, M. Liu, M. Hatano, M. Uchiyama,  $\text{BaZr}_{0.1}\text{Ce}_{0.7}\text{Y}_{0.2}\text{O}_{3-\delta}$  as an electrolyte for low-temperature solid-oxide fuel cells, *Adv. Mater.* 18 (2006) 3318.
- [64] D. Han, X. Liu, T.S. Bjørheim, T. Uda, Yttrium-doped barium zirconate-cerate solid solution as proton conducting electrolyte: why higher cerium concentration leads to better performance for fuel cells and electrolysis cells, *Adv. Energy Mater.* 11 (2021) 2003194.
- [65] D. Pergolesi, E. Fabbri, A. D'Epifanio, E. Di Bartolomeo, A. Tebano, S. Sanna, S. Licocchia, G. Balestrino, E. Traversa, High proton conduction in grain-boundary-free yttrium-doped barium zirconate films grown by pulsed laser deposition, *Nat. Mater.* 9 (2010) 846.
- [66] Z. Luo, Y. Zhou, X. Hu, N. Kane, T. Li, W. Zhang, Z. Liu, Y. Ding, Y. Liu, M. Liu, Critical role of acceptor dopants in designing highly stable and compatible proton-conducting electrolytes for reversible solid oxide cells, *Energy Environ. Sci.* 15 (2022) 2992.
- [67] Z. Luo, Y. Zhou, X. Hu, N. Kane, W. Zhang, T. Li, Y. Ding, Y. Liu, M. Liu, Highly conductive and durable Nb(Ta)-doped proton conductors for reversible solid oxide cells, *ACS Energy Lett.* 7 (2022) 2970.
- [68] Z. Luo, Y. Zhou, X. Hu, W. Wang, Y. Ding, W. Zhang, T. Li, N. Kane, Z. Liu, M. Liu, A new class of proton conductors with dramatically enhanced stability and high conductivity for reversible solid oxide cells, *Small* 19 (2023) e2208064.
- [69] K. Saito, M. Yashima, High proton conductivity within the "Norbby gap" by stabilizing a perovskite with disordered intrinsic oxygen vacancies, *Nat. Commun.* 14 (2023) 7466.
- [70] G. Weng, S. Lei, R. Wang, K. Ouyang, J. Dong, X. Lin, J. Xue, L.-X. Ding, H. Wang, A high-efficiency electrochemical proton-conducting membrane reactor for ammonia production at intermediate temperatures, *Joule* 7 (2023) 1333.
- [71] Z. Zhu, B. Liu, J. Shen, Y. Lou, Y. Ji,  $\text{La}_2\text{Ce}_2\text{O}_7$ : a promising proton ceramic conductor in hydrogen economy, *J. Alloy. Compd.* 659 (2016) 232.
- [72] B. Choudhary, L. Besra, S. Anwar, S. Anwar,  $\text{La}_2\text{Ce}_2\text{O}_7$  based materials for next generation proton conducting solid oxide cells: progress, opportunity and future prospects, *Int. J. Hydrog. Energy* 48 (2023) 28460.
- [73] I. McPherson, J. Zhang, Can electrification of ammonia synthesis decrease its carbon footprint? *Joule* 4 (2020) 12.